Signal Processing Evaluated by Allan and Hadamard Variances

J. Skřínský, M. Skřínská, and Zdeněk Zelinger

***Abstract*—**Laser spectrometry offers high sensitivity and broad dynamic range, permitting monitoring of concentrations from trace values to the saturation level. Such techniques are increasingly used for field laser applications in industry and research. Photoacoustic spectrometry has been used as an in situ method for observation of actual concentrations combined with high spatial and time resolution. Photoacoustic spectrometry is based on the photoacoustic effect and in conjunction with lasers has already been used in monitoring of industrial trace gas components at ppb concentrations. It has been proven that the characteristic of laser frequency/wavelength stability is critically important for evaluation of metrology system performance when the function principle is based on photoacoustic spectrometry. In particular, the long-term stability range, corresponding to noise in the hundreds of hertz to kilohertz bandwidth, strongly affects the measurement final accuracy at the reported measurement rates. We reported trace gas measurements performed by photoacoustic technique and we determined the time domain stability criteria for laminar and turbulent flows measured in the street canyon model. The preliminary evaluation of the instrument performance was performed by in situ measurements of unstable O_3 and stable CH_3OH light pollutant concentrations. Further, the instrument has been adapted to in situ measurements of C_2H_5OH trace gas concentrations. We have determined optimal averaging times for O_3, CH_3OH and C_2H_5OH measured at static operation connected to wind tunnel. The Allan and Hadamard variance methods were used for stability analysis.

***Keywords*—**Allan variance, Hadamard variance, Photo-acoustic spectroscopy, Trace gas sensing

I. Introduction

THE photo-acoustic spectrometry is selective, sensitive, and nondestructive laser-based analytical method. This method has been steadily more employed to physical modeling of trace amounts of pollutant gases present in the atmosphere.

This work was supported in part by the project Opportunity for young researchers, reg. no. CZ.1.07/2.3.00/30.0016, supported by Operational Programme Education for Competitiveness and co-financed by the European Social Fund and state budget of the Czech Republic and in part by the project Innovation for Efficiency and Environment, reg. no. CZ.1.05/2.1.00/01.0036 supported by Operation Programme Research and development for Innovation and financed by the Ministry of Education, Youth and Sports.

J. Skřínský is with the Energy Research Centre, VŠB-TU Ostrava, 17. listopadu 15/2172, 700 30, Ostrava, Czech Republic (corresponding author to provide phone: + 420597324936; e-mail: skrinsky.jan@vsb.cz).

M. Skřínská is with the Energy Research Centre, VŠB-TU Ostrava, 17. listopadu 15/2172, 700 30, Ostrava, Czech Republic (e-mail: maria.skrinska@vsb.cz)..

Z. Zelinger is with the Department of Spectroscopy, J. Heyrovsky Institute of Physical Chemistry, Dolejškova 2155/3, 182 23 Prague 8, Czech Republic (e-mail: zdenek.zelinger@jh-inst.cas.cz).

The output data of all spectrometric measurements are often obscured by various noises which negatively influence the instrument sensitivity.

An improvement of sensitivity of the photo-acoustic spectrometer depends on the determination of optimal integration time. Allan variances method becomes a standard procedure for evaluation of optimal integration time of the tunable diode-laser absorption instrument. In the present contribution an approach for investigation of optimal integration time for CO_2 laser photo-acoustic spectrometry is described for the minimum detectable concentration of O_3, CH_3OH and C_2H_5OH molecules.

Photo-acoustic spectrometer with CO_2 laser used for field applications in industry and research was adapted for detection of two light atmospheric pollutants (CH_3OH, C_2H_5OH).

Two- and three-sample variances of the photoacoustic signal have been utilized to test the short- and long-term stability of the spectrometer based on the mathematical evaluation of the calculated signal-to-noise ratios of absorption spectra. An approach for studies of the influence on the optimal averaging time as well as the comparison of different variance families for the minimum detectable concentrations is described in [1].

II. Previous studies

While the stability characterizations of tunable diode-laser absorption instruments by Allan variance have been published starting from 1993, the information on the application of Allan and Hadamard variances on CO_2 laser photo-acoustic spectrometry and other techniques for trace gas concentration measurements is rather scarce.

In 1989 was the Allan variance first utilized on photo-acoustic spectrometer with CO_2 laser using Lamb-dip from a photoacoustic cell [2]. CO_2 laser was used to optically pump a CH_3OH laser stabilized at the center of the CH_3OH absorption line. The frequency stability of the CO_2 laser was measured in terms of the Allan variance as $\sigma(\tau) = 3 \times 10^{-9}\ \tau^{-1/2}$ ($1 < \tau < 100$ s).

Later, the stability tests of photo-acoustic spectrometer with tunable diode laser were described based on a cantilevered technique for sensitive detection of molecular oxygen [3]. The detection limit obtained was 5000 ppm.

The third study was on CO_2 detection using near infrared (NIR) diode-laser based wavelength modulation photoacoustic spectroscopy. An integration time of app. 100 s was selected for the detection-limit [4].

There have been also other laser-based detection systems for gas phase detection tested by the Allan variance method. It was presented the measurement of atmospheric N_2O and CH_4 using mid-infrared quantum cascade laser combined with astigmatic multipass cell. From the Allan variance analysis of 0.06 ppb of N_2O and 0.7 ppb of CH_4 they obtained the optimal integration times of app. 100 and 200 s [5].

Similarly in 2007 measurements of atmospheric N_2O and CH_4 was presented using quantum cascade laser spectroscopy. Obtained optimal integration time was app. 200 s for app. 0.5 ppb of N_2O, and app. 2.9 ppb of CH_4 [6].

In 1996 the analysis of 0.075 ppm NO was described. It was measured by quantum cascade laser combined with astigmatic multipass cell with the optimal integration time calculated as app. 80 s. detected the value of app. 0.01 mmol atmospheric concentration of OCS by quantum cascade laser combined with white-type multi-pass cell. From the measured calculated results it was derived optimal integration time 138 s [7].

III. Experiment

The photoacoustic spectrometer used has been described in detail [10],[11],[12],[13]. Briefly, it consists of a single-pass absorption system connected with the aerodynamic tunnel. By laser modulation unit modulated IR photon beam emitting from CO2 laser was externally modulated by chopper. The beam was directed into the photoacoustic cell and after the passing the cell it was focused to the pyro-detector. For the control of the position of emission lines of CO_2 laser was used spectral analyzer (type 16-A, Optical Engineering Inc.). Cylindrical photoacoustic cell (inner diameter 8 mm, length 380 mm) was temperature stabilized (app. 30 ˚C). Acoustic wave was detected in the absorption cell by using the electret microphone placed in the middle of the full length of the absorption cell. Measured modulated signal was demodulated by lock-in nanovoltmeter (type 232, UNIPAN, Warsaw, Poland). The measured concentration of the methanol was generated by permeation method. As permeation standards were used methanol and ethanol (light pollutants; company: Sigma Aldrich; purity: 99.7%). Both methanol and ethanol samples were generated by permeation method. Permeation standards were placed in the temperature stabilized chamber (23.0 ± 0.6 °C). A constant flow rate of carrier gas (3.1 ± 0.1 m.s-1) passed through a chamber. Flow rate was measured with the sample drawn through a photoacoustic tube and then through the flow meter. The flow of the buffer gas through the chamber was regulated to small constant flow rate value approximately 1 $m.s^{-1}$ and was pumped into the photoacoustic cell together with the measured sample. From the cell it was directed into the pump through the flow rate regulator. Whole experiment i.e. modulation frequency of the chopper and modulation frequency of the CO_2 laser and the acquisition of the data was computer controlled. For the long time scan measurements were selected isolated line of CH_3OH, C_2H_5OH at CO_2 laser emission line of wavenumber 1045.0413 cm^{-1} (9P (22)).

IV. Analysis

The analysis procedure made by variance based method for laser-based systems has been described in detail by [1]. The measured data are often affected by systematic effects such as frequency offset and linear frequency drift that, if not properly estimated and removed, will distort the power spectral density estimate which is an important characteristic for determining different noise types. In such a case instead of the frequency measurement the time domain measurement takes place over a finite time interval. For a formal description of the stability of described spectrometer in the time domain we assume a recorded set of N time-series data referring to amplitude or frequency stability represented by x_i (i = 1 ... N) elements. These data sets are usually described by its average value A and the variance σ^2. In general, the N elements of the original data set can be divided into M subsets containing k elements (M = N/k). For each of these M subsets average value A_n and a simple variance σ_n^2 can be calculated. The calculation of the expected value for the time average of simple Allan (two-sample) variance $\langle\sigma^2_A(k)\rangle t$ is defined for a set of m-1 independent measurements to obtain a more precise estimate for the detection limit. The assumption for this calculation is that data set is sorted according to the measurement time.

Subset average value for measured elements $A_s(k)$ is given by:

$$A_s(k) = \frac{1}{k}\sum_{l=1}^{k} x_{(s-1)k+l} \tag{1}$$

Allan variance for measured elements $\langle\sigma^2_A(k)\rangle t$ is defined as:

$$\left\langle \sigma_A^2(k) \right\rangle_\tau = \frac{1}{2(m-1)}\sum_{s=1}^{m-1}[A_{s+1}(k) - A_s(k)]^2 \tag{2}$$

$\langle\sigma^2_A(k)\rangle t$ is the time average of Allan variance [a.u.]; A_S is the arithmetical mean of elements [a.u.]; k is a number of averages [-]; m is a number of subsets; N is a total number of elements [-]; τ is integration time [s]; s, l are the indexes (s = 1, …, m – 1 and l = 1, …, k).

The Hadamard (three-sample) variance examines the third difference in elements, equivalent to the second difference of the time-averaged frequencies over three successive adjacent time intervals. As a spectral estimator, the Hadamard transform has higher resolution than the Allan variance, since the equivalent noise bandwidth of the Hadamard and Allan spectral windows are $1.2337N^{-1}\tau^{-1}$ and $0.476\tau^{-1}$ respectively. For the purposes of time-domain frequency stability characterization, the most important advantage of the Hadamard variance is its insensitivity to linear frequency drift, making it particularly useful for the analysis of rubidium atomic clocks. It has also been used as one of the components of a time-domain multi-variance analysis.

Hadamard variance for measured elements $<\sigma^2_H(k)>_t$ is defined as:

$$\left\langle \sigma_H^2(k) \right\rangle_\tau = \frac{1}{6(m-2)} \sum_{s=1}^{m-2} (A_{s+2}(k) - 2A_{s+1}(k) + A_s(k))^2 \quad (3)$$

$<\sigma^2_H(k)>_t$ is the time average of Hadamard variance [a.u.], AS is the arithmetical mean of elements [a.u.], k is a number of averages [-], m is a number of subgroups, N is total number of elements [-], t is an integration time [s], s, l are the indexes (s = 1, …, m – 2 and l = 1, …, k).

In the frequency domain the data is often affected by systematic effects such as frequency offset [14]. Therefore, the frequency stability is more easily specified through the characterization in the time domain.

For the simple Allan variance, the transfer equation has the form:

$$\left\langle \sigma_A(k) \right\rangle_\tau = 2 \cdot \sum_0^\infty S_y(f) \cdot \frac{\sin^4(\pi \cdot \tau \cdot f)}{(\pi \cdot \tau \cdot f)} \cdot df \quad (4)$$

For the simple Hadamard variance, the transfer equation has the form:

$$\left\langle \sigma_H^2(k) \right\rangle_\tau = 16 \cdot \sum_0^\infty S_y(f) \cdot \frac{\sin^6(\pi \cdot \tau \cdot f)}{(\pi \cdot \tau \cdot f)} \cdot df \quad (5)$$

The mathematical form of power spectral density estimate:

$$S_y(f) = \sum_\alpha h_\alpha f^\alpha \quad (6)$$

α is an integer that runs from -2 to 2, h_α is the transfer function proportional to the power of α.

The frequency domain is characterized by five noise categories: (1) white phase noise, (2) flicker phase noise, (3) white frequency noise, (4) flicker frequency noise and (5) random walk frequency noise [14]. This model adequately describes most of the observed noise processes. These five noise categories are grouped into three parts, thus the integral calculation can also be spread into three independent parts and the result is the sum of these fractional calculations:

$$\left\langle \sigma_H^2(k) \right\rangle_\tau = c_{white-noise} + c_{1/f} + \sum_\alpha c_{drift,\alpha} \tau^\alpha \quad (7)$$

$<\sigma^2_A(k)>t$ is the Allan variance [a.u.], $c_{white-noise}$ is a constant characterizes white noise [a.u.], $c_{1/f}$ is a constant characterizes flicker noise, $\Sigma C_{drift,\alpha}\tau^\alpha$ characterizes the type of the system drift [-], τ is the integration time.

V. RESULTS AND DISCUSSIONS

The results of application of both approaches are analyzed in terms of system stability and detection limit. The system stability is an important figure of merit as it determines the maximum allowable time in which statistically independent data may be averaged in order to reduce noise and thus improve the detection limit.

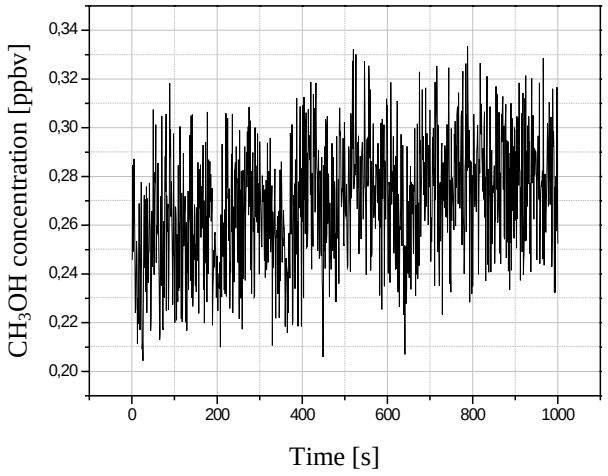

Fig. 1 Methanol concentration in ambient air recorded during wind tunnel large scale measurement (mass flow rate of approx. 1.0 $m.s^{-1}$) - „trends“ on 1000 s time-scale

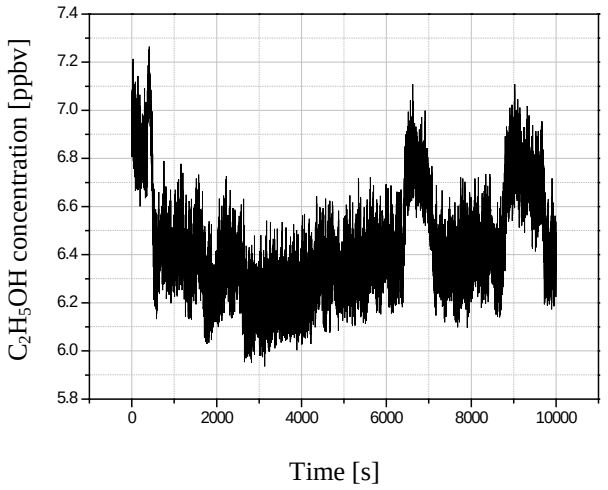

Fig. 2 Ethanol concentration in ambient air recorded during the wind tunnel large scale measurement (mass flow rate of approx. 1.5 $m.s^{-1}$) - „trends“ on 1000 s time-scale

An ambient time series is shown in Fig. 1-2, where sample of both methanol and ethanol have been recorded at 1045.0413 cm^{-1} for about 1000 s. By using the equations 4-5 we are able to make the transformation of the time domain spectrum into the frequency domain and vice-versa.

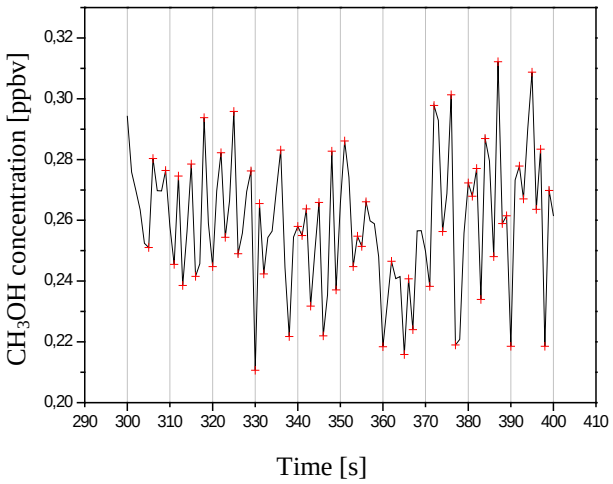

Fig. 3 Frequency dependence of methanol concentration in the Fourier spectrum - „trends“ in the inertial 100 s subrange.

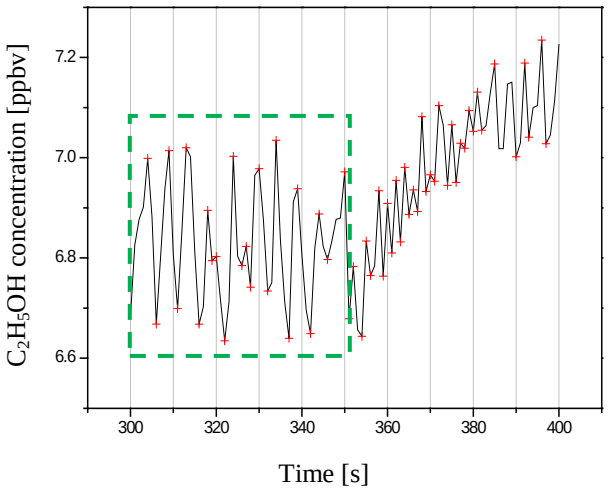

Fig. 4 Frequency dependence of ethanol concentration in the Fourier spectrum - „trends“ in the inertial 100 s subrange

Frequency spectrum of the time series is not displayed. From the pre-evaluation expected random walk noise (α = -5) frequency dependence in the inertial subset is expected. A closer look into short intervals of the time series resolved at 1045.0413 cm^{-1} for 100 s time interval is shown in Fig. 3-4. At this scale (non-linear and linear) short-term 'trends' can be observed due to turbulence in the inertial subset and therefore a similar behavior with respect to averaging can be expected as for the long-term drift already discussed. Such behavior is especially depicted in Fig 4 by the dashed line. A closer analysis of the time series between 300 s and 400 s in Fig. 4 with equivalent mass flow rate indicate a different concentration trends in compare to Fig. 3. As a consequence further long-term dependence should provide the information about this instability in the over all stability analysis.

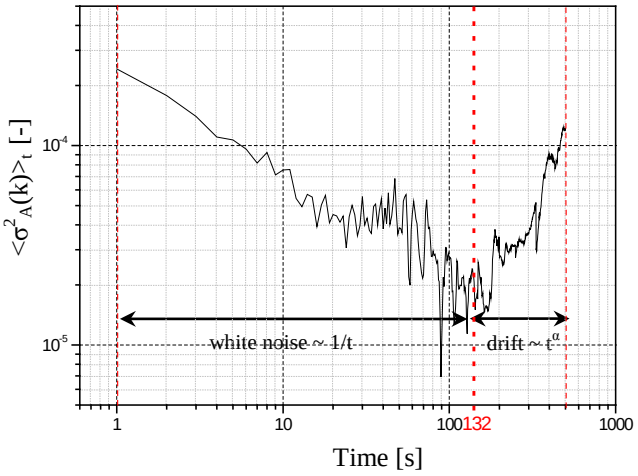

Fig. 5 The σ/τ plot for the methanol measurements includes features in of the frequency spectrum above, but also provides information about the long-term (1000 s) behavior.

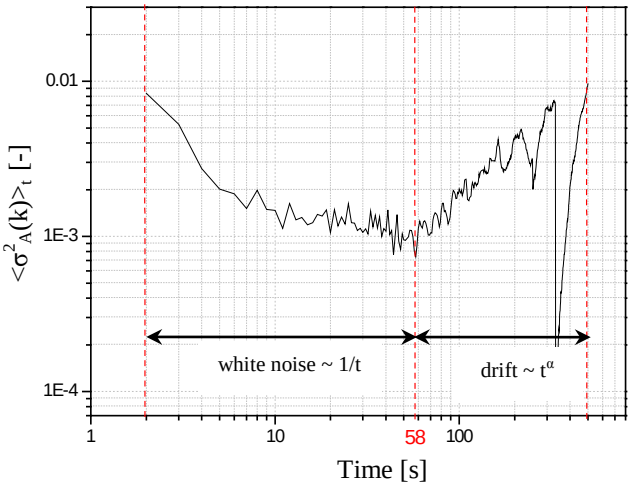

Fig. 6 The σ/τ plot for the ethanol measurements includes features in of the frequency spectrum above, but also provides information about the long-term (1000 s) behavior

The time-domain characterization based on a two-sample variance using an σ/τ plot shown in Fig. 5-6 provides the same information as the spectral characteristics of turbulence in the frequency domain. There is no turbulence (not frequency dependent process) resolved for averaging intervals below 20 s ($f^{-5} \leftrightarrow \tau^{+2}$) depicted by continually decreasing line. First small turbulence is resolved for averaging interval for 20-40 s and appears as a drift seen on a time scale at this inertial sub-range. The small high-frequency damping can also be identified for short (40-60 s) integration times. For increasing averaging times (90–200 s) flicker noise from the laser and electronic components dominate and the two-sample variance remains at approximately constant level ($f^{-1} \leftrightarrow \tau^{0}$). White noise dominates at longer integration time because fast fluctuations contribute less to the variance and averaging leads to a decreasing

variance. At the approximately 132 s time scale the two-sample variance approaches the white noise limit. Fig. 9,11 give an estimate of the ultimate sensitivity which can be achieved as a function of integration time. Further turbulences are resolved for averaging interval at approximately 150-200 s, 300-350 s and 400-450 s and appear as a drift seen on a time scale with higher α value than average.

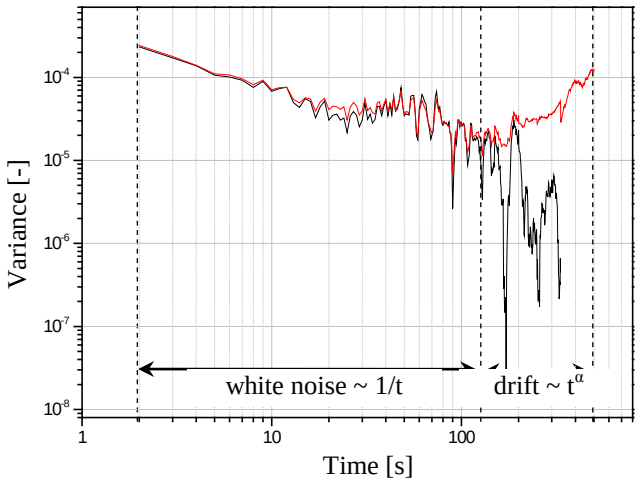

Fig. 7 The results of full analysis for 1000 data points and all-averages, all-number of subsets

For calculation of fully resolved Allan and Hadamard variances for 1000 s time interval we repeated the following procedure. First, we have pre-evaluated the measured data sets for methanol using software ALAVAR 5.2. Using this software with the limited time resolved output (1, 2 4, 8, 16, 32, 64, 128, 256) without possibility to change the number of averages (k) and subsets (m) all of the plots appeared as partly resolved. As a result of this pre-analysis we obtained the approximate assignment of optimal integration times and approximate assignment of noise figures. Consequently these datasets for individual measurements were analyzed by all-averages all-number of subsets analysis using the algorithm described in an analysis part above (see equations 1-7). By repeating this procedure we evaluated a total of 10 data sets obtained at a time interval of 1000 s and obtained an averaged value of optimal integration time by two different procedures lying in the interval from 120 to 140 s. According to Fig. 7, Hadamard variance is convergent for $\alpha > -5$, unlike the Allan variance, which is convergent for $\alpha > -3$ (from the last term of equation 7). Thus it would be possible to use the Hadamard variance to probe for noise beyond random walk frequency modulation.

Moreover, the Hadamard variance is unaffected by linear frequency drift. This makes it an excellent tool for investigating of those noise types, whose signatures are similar to and often confused with linear drift. Both Allan and Hadamard variances are not sensitive to the deterministic content.

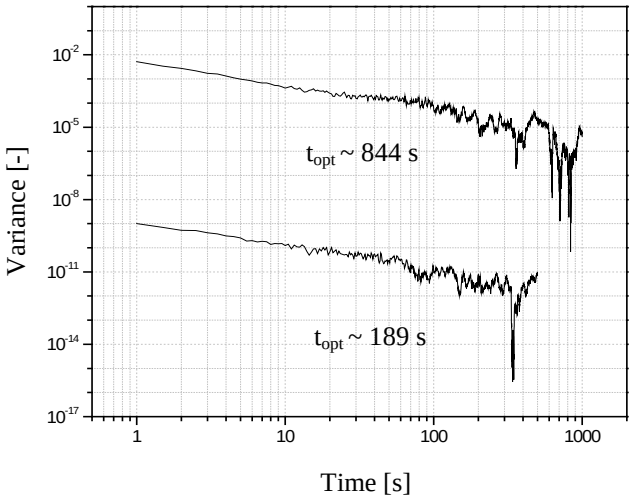

Fig. 8 First-stage Allan-plot for blind measure (upper curve), laminar flow (app. 1.0 m/s) of ethanol (lower curve)

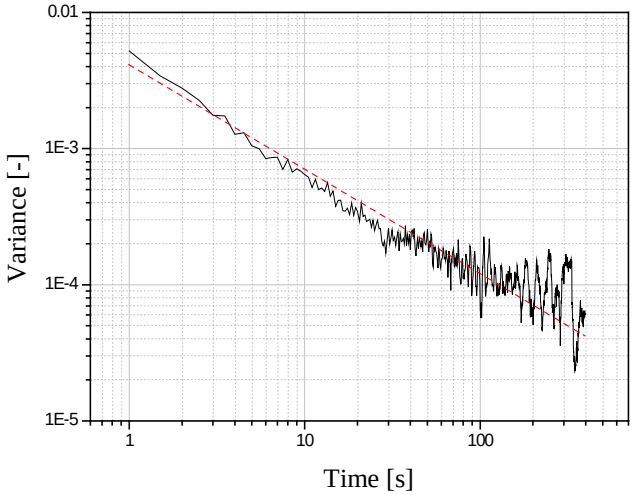

Fig. 9 Second-stage Allan-plot for optimal integration time of 346 s

In Fig. 8-9 is shown an example of a data set evaluated by the Allan variance calculation obtained at a time interval of 2000 s (upper curve for blind measure) and 1000 s (lower curve for laminar flow). The obtained optimum integration times are characteristic for a given instrument at given experimental conditions and reflect the overall system stability. They were obtained on the basis of Allan variance and lie in the minimum of the Allan-plot. At low integration times White noise ($\langle\sigma^2_A(k)\rangle_t \sim 1/t$) dominates. After the optimal integration time the influence of the linear drift $\langle\sigma^2_A(k)\rangle_t \sim ta$, a = 1-2) starts.

The Allan-plots in Fig. 8-9 are the main results of the testing of considered flows systems applied in the photoacoustic detection of ethanol. The optimal integration time (as a result of 4 measurements at the given experimental conditions) for laminar flow lies at interval value of 100 s - 200 s and the optimal integration time for turbulent flow lies at interval value 300 s - 400 s. The difference between the laminar and

turbulent flows is approx. 100 s - 300 s. If the data are acquired with the integration time equal to the optimum integration time the system drift will less significantly influenced the quality of output data. After such a drift correction the data can be stored and analyzed again in the terms of Allan variance and made into second stage Allan-plot. Fig. 8-9 gives an estimate of the ultimate sensitivity, which can be achieved as a function of integration time. In Fig. 8a the measured Allan variance is of positive slope if the measured integration time is higher than 844 s.

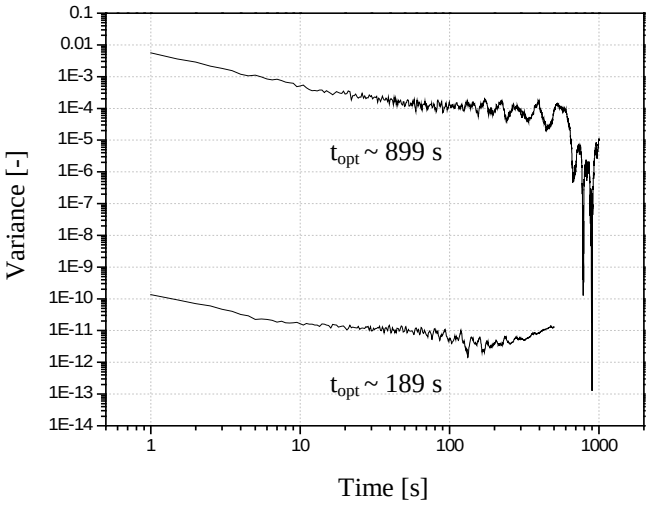

Fig. 10 First-stage Allan-plot for blind measure (upper curve), laminar flow (app. 1.2 m/s) of methanol (lower curve)

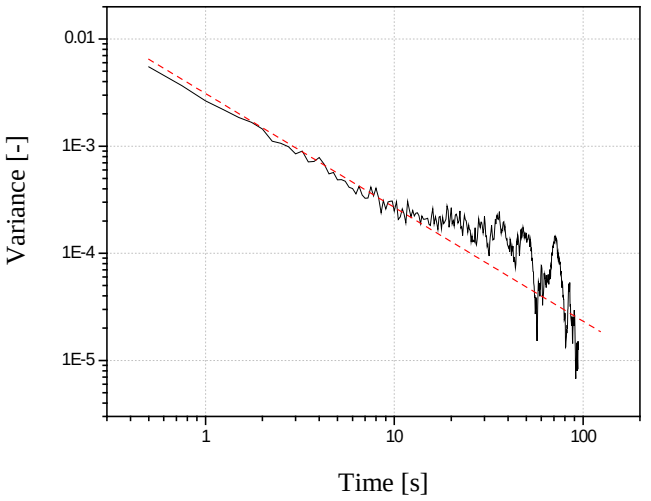

Fig. 11 Second-stage Allan-plot for optimal integration time of 189 s

The measured Allan variance is of negative slope when the measured integration times are lower than 346 s. These slope changes in the inertial integration time interval, in which wavenumber fluctuates according to the type of noise, dominate the Allan-plot. The similar trend could be recognized in Fig. 8 (lower curve) shows the second stage Allan-plots for optimal integration times with white noise dominated part of Allan-plots with the typical decreasing tendency (dashed line). The white noise is suppose to be produced in the tested system mainly by detectors sensor and with the knowledge that the value of white noise depends upon the temperature of the circuit could be the possible slope tendency explained by the thermal fluctuations and the respective change of the movement velocity of charged particles in the sensor. Or alternatively by the non-uniform arrival of acoustic waves at a detector sensor caused the fluctuations that might be counted [1]. Which of these two alternatives dictates the slope of white noise depends on the actual conditions influencing the white noise generation.

VI. Conclusion

This study conducted with the previous studies [1], [15] introduces step-by-step development of a methodology for the evaluation of the optimal integration times. It was demonstrated that both σ/τ plots provide information about the optimum averaging time for tested detection systems. A principle of approach and the preliminary study on the O_3, CH_3OH and C_2H_5OH molecules analyzed by two- and three-sample variance for the minimum detectable concentration of pollutant (down to ppb) is shown. This permit makes a systematic comparison for derived integration time parameters of different e.g. $C_nH_{2n+1}X$ (n=1-2, X=OH) environmental pollutants analogues. The concept of Allan and Hadamard variance has been utilized for the stability and sensitivity analysis of described experimental apparatus. Calculated variances plotted as a function of integration time (t) give the first stage σ/τ plot. The σ/τ plots demonstrate the noise influences on the investigated system (see Fig. 7). The optimal integration times for the detection of trace-gas concentrations were determined by the combination of Allan and Hadamard variance methods. The analysis of Allan and Hadamard variances was demonstrated on a detection of gaseous CH_3OH and C_2H_5OH by CO_2 laser photo-acoustic spectrometer with a given noise curve in the time domain. The analyzed signal was subtracted from the reference one, time dependent time fluctuations were obtained, and Allan and Hadamard variances were calculated. The presented approach contributes to the analysis of performance of a CO_2 laser detection systems described and it is possible to improve the signal to noise ratio in one order. The σ/τ plots provide information about the optimum averaging time for the tested system. It is the case of detection of species under different flow regimes.

Acknowledgment

Authors would like to thanks to the project Opportunity for young researchers, reg. no. CZ.1.07/2.3.00/30.0016, supported by Operational Programme Education for Competitiveness and co-financed by the European Social Fund and the state budget of the Czech Republic and to the project Innovation for Efficiency and Environment, reg. no. CZ.1.05/2.1.00/01.0036 supported by Operation Programme Research and development for Innovation and financed by the Ministry of Education, Youth and Sports.

REFERENCES

[1] Werle, P., Mücke, R., Slemr, F., The limits of signal averaging in atmospheric trace-gas monitoring by tunable diode-laser absorption spectroscopy, *Applied Physics B*, Vol. 57, No 2, 1993, pp. 131-139.

[2] Yanm, H., Kurosawam, T., Onaem, A., Frequency stabilization of a CO_2 laser using Lamb-dip from a photo-acoustic cell, *Optics Communications*, Vol. 73, No.2, 1989, pp. 136-140.

[3] Cattaneo, H., Laurila, L., Hernberg, R., Photoacoustic detection of oxygen using cantilever enhanced technique, *Applied Physics B*, Vol. 85, No. 2-3, 2006, pp. 337–341.

[4] Li, J., Liu, K., Zhang, W., Carbon dioxide detection using NIR diode laser based wavelength modulation photoacoustic spectroscopy, *Optica Applicata*, Vol. 38, No. 2, 2008, pp. 341-352.

[5] Nelson, D. D., Mcmanus, A, B., Urbanski, S., Herndon, S., Zahniser, M. S. High precision measurements of atmospheric nitrous oxide and methane using thermoelectrically cooled mid-infrared quantum cascade lasers and detectors. *Spectrochimica Acta Part A*, 2004, Vol. 60, No. 14, pp. 3325–3335.

[6] Kroon, P. S. - Hensen, A. - Jonker, H. J. J. - Zahniser, M. S. - Van 'Tveen, W. H. - Vermeulen, A. T. Suitability of quantum cascade laser spectroscopy for CH_4 and N_2O eddy covariance flux measurements. *Biogeosciences*, 2007, Vol. 4, No. 5, pp. 715–728.

[7] Stimler, K. - Nelson, D. - Yakir, D. High precision measurements of atmospheric concentrations and plant exchange rates of carbonyl sulfide using mid-IR quantum cascade laser. *Global Change Biology*, 2009, pp. 1-8.

[8] Skřínský, J., Janečková, R., Grigorová, E., Allan variance for optimal signal averaging monitoring by diode-laser and CO_2 laser photo-acoustic spectroscopy, *Journal of Molecular Spectroscopy*, Vol. 256, No. 1, 2009, pp. 99–101.

[9] Baugh, R.A., Frequency modulation analysis with the Hadamard variance, *25th Annual Symposium on Frequency Control*, 1971, pp. 222-225.

[10] Zelinger, Z., Jančik, I., Engst, P, Measurement of the NH_3, CCl_2F_2, $CHClF_2$, $CFCl_3$, and $CClF_3$ absorption coefficients at isotopic $^{13}C^{16}O_2$ laser wavelengths by photoacoustic spectroscopy, *Applied Optics*, Vol. 31, No. 33, 1992, pp. 6974-6975.

[11] Zelinger, Z., Střižík, M., Kubát, P., Quantitative analysis of trace mixtures of toluene and xylenes by CO_2 laser photoacoustic spectrometry, *Analytica Chimica Acta*, 2000, Vol. 422, No. 2, pp. 179–185.

[12] Zelinger, Z., Střižík, M., Kubát, P., Laser remote sensing and photoacoustic spectrometry applied in air pollution investigation, *Optics and Lasers in Engineering*, Vol. 42, No. 4, 2004, pp. 403–412.

[13] Herecová L., Hejzlar T., Pavlovský J., CO_2-laser photoacoustic detection of gaseous n-pentylacetate, *Journal of Molecular Spectroscopy*, Vol. 256, No. 1, 2009, pp. 109-110.

[14] Todd, W., A multi-variance analysis in the time domain, *The 24th Annual Precise Time and Time Interval (PTTI) - Applications and Planning Meeting*, 1992, pp. 413-426.

[15] Skřínský, J., Skřínská, M., Zelinger, Z. Calculation, simulation and experimental validation of Allan and Hadamard Variance. In Proceedings of the 2nd International Conference on Energy Systems, Environment, Entrepreneurship and Innovation (ICESEEI ´13), 2013, pp. 75-81.